Title X-IFU CryoAC geometrical and detection efficiencies.

Prepared by :	Simone Lotti, Claudio Macculi, Andrea Argan	Date	:	31/07/2019
Inputs by :		Date	:	
Checked by :	Daniele Brienza	Date	:	31/07/2019
Agreed by :	Andrea Argan 	Date	:	31/07/2019
Authorised by:	Luigi Piro	Date	:	31/07/2019

DISTRIBUTION LIST

X-IFU consortium
ESA

DOCUMENT CHANGE RECORD

Issue	Date	Changed Section	Description of Change
1	31/07/2019		1st Issue

Abbreviations and acronyms

Item	Meaning
AIT	Assembly Integration and Test
ASI	Agenzia Spaziale Italiana
ASW	Application Software
CADM	Configuration and Data Management
CNR	Consiglio Nazionale delle Ricerche
CPO	Central Project Office
CryoAC	Cryogenic Anticoincidence
FA	Funding Agency
FEE	Front End Electronics
FPA	Focal Plane Assembly
GSE	Ground Segment
ICU	Instrument Control Unit
INAF	Istituto Nazionale di Astrofisica
LPO	Local Project Office
MP	Management Plan
OBS	Organization Breakdown Structure
PA	Product Assurance
PBS	Product Breakdown Structure
PS	Project Scientist
SM	System Manager
UniGE	University of Genova
UniPA	University of Palermo
WBEE	Warm Back End Electronics
WBS	Work Breakdown Structure
WEE	Warm Electronics
X-IFU	X-ray Integral Field Unit

Applicable Documents

[AD#]	Doc. Reference	Issue	Title
[AD1]			
[AD2]			
[AD3]			
[AD4]			

Reference Documents

[RD#]	Doc. Reference	Issue	Title
[RD1]			
[RD2]			
[RD3]			
[RD4]			
[RD5]			
[RD6]			

Table Of Contents

1 NXB VS DISTANCE VS CRYOAC SIZE

It has not ever been possible to perform the exercise NXB vs CryoAC distance/size on the full mass model, since it would have required over 9 simulations (5 for distance, 4 for size), each simulation requiring ~ 10 days (computing time + data analysis), for a total of at least 3 months (assuming no dead time between one simulation and the following one), and only for the GCR protons component (not alphas, not electrons).

Thus, for the primaries component, since the particles can be seen as "traces", and since having high energy more or less by crossing the cryostat loose a very small amount of it, we performed the exercise by using a quite reduced mass model (an aluminum and Niobium spheres 15 mm and 0.5 mm thick, respectively, surrounding the detectors) with a huge gain in computational time. Indeed, the NXB due to only primaries from the full MM and the result from the spheres related for the same CryoAC-to-TES array distance/size is compatible even though, due to the CryoAC efficiency in rejecting the primaries, the statistics is still poor.

Then, by the spheres model, we have also probed the rejectable secondaries, thus generating the attached 3 plots (Fig. 1, Fig. 2, Fig. 3) of percentage variation of the residual counts with respect to the baseline configuration (1 mm distance, CryoAC to TES array area 4.91/2.35 cm^2/cm^2). In general, unlike the primaries that are not particularly influenced, the absolute level of secondaries-induced background is not reliable, due to the very much different MM. Hence, while the spheres model cannot provide definitive results about the expected absolute value of the NXB, such a simple model can give some hints in assessing the “variation” of the residual counts by moving the geometrical parameters as the distance and the CryoAC size.

By chance, we also see that a huge revision of the mass model (from full to spheres) provides a decrease of the NXB by a factor ~ 4 (if you evaluate the NXB obtained by the sphere for the baseline configuration you get 1.4E-3 cts/cm2/s/keV with respect to 6E-3 cts/cm2/s/keV from the full MM, without passive shielding in both cases): this can give us a reference upper limit about the impact in revising the MM, since it represents the most dramatic revision possible to the MM.

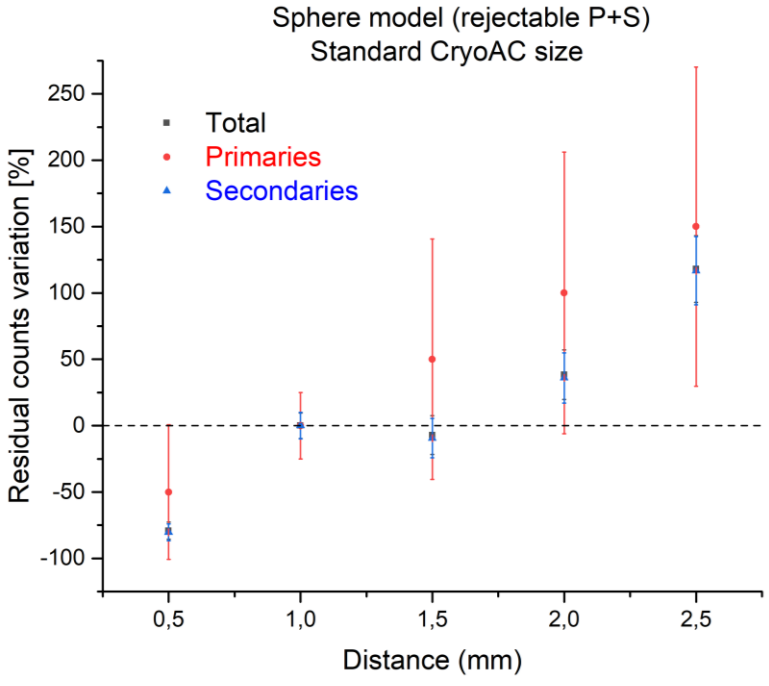

Fig. 1 - Residual counts variation vs distance between the CryoAC and the TES array.

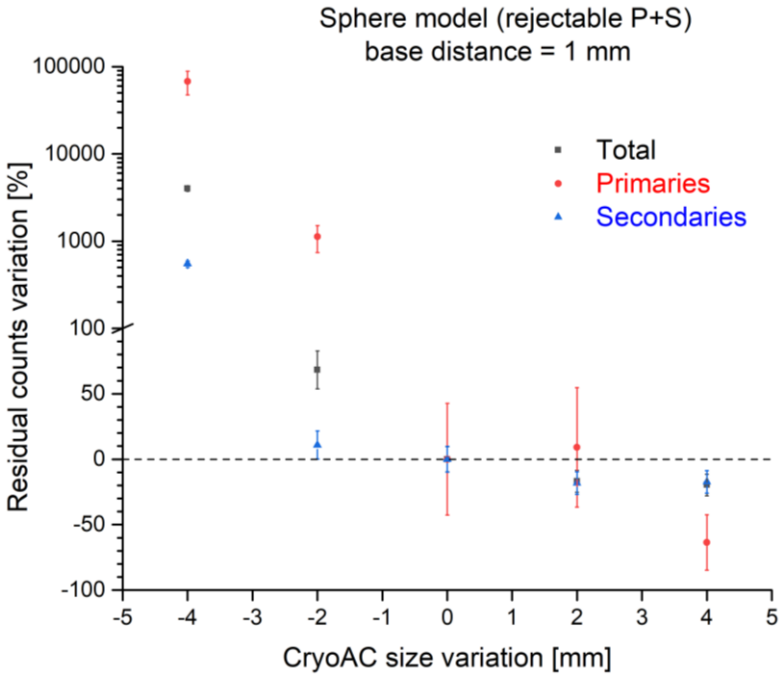

Fig. 2 - Residual counts variation vs CryoAC size.

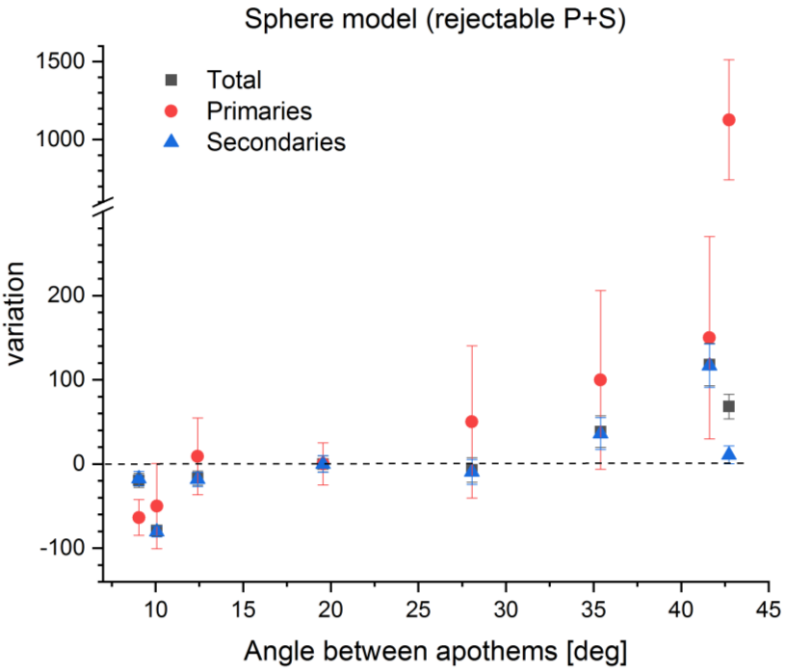

Fig. 3 - Variation vs angle between apothems.

The plot of the Total counts seems to follow the secondaries one since the secondaries represent the major fraction of the residual counts.

So, to justify the current CryoAC design, from the spheres model we see that 1 mm distance and 4.91 cm2 CryoAC area (size variation = 0) represents a reasonable starting point for the simulations

with the full MM (we do not take 1.5 mm distance to have some margin, and larger areas do not affect sensibly the residual counts variation but only the detector complexity).
With these assumptions, we get an NXB compliant with the requirement in the full MM.

So, assuming all detector pixels contained into an hexagon of r=10.5 mm, such a geometry defines an angle of 17.1 deg between the vertices of the 2 detectors (so considering radii) or, equivalently, an angle of 19.56 deg between the edges of the 2 detectors (so considering apothems). So we can rephrase the "Geometrical" requirement as follows:

> "**The CryoAC shall intercept all directions passing through the TES array with an angle > 19.56 deg from the detector surface.**"

This way, the requirement is purely geometric: we report “directions” and not “particles”. Doing so, the compliance with this requirement “as written” can be verified just from the CAD, and it is not necessary any experimental test.

2 FOR COMPLETENESS: CRYOAC LOW ENERGY THRESHOLD AND DETECTION EFFICIENCY

Here below (Fig. 4) we show the residual NXB (integrated over 2-10 keV bandwidth) vs the CryoAC low energy threshold, due to particles (primaries and secondaries) interacting with the main array but not triggering the CryoAC (i.e. not interacting with the CryoAC or interacting with CryoAC but deposing energy lower than the threshold). The analysis has been carried out on the full mass model compliant with the newly above-specified requirement.
As shown, the secondaries are the component driving the choice of the CryoAC low energy threshold
By allocating the amount of 2/10 of the required NXB, which is 8E-3 cts/cm^2/s, to the total unrejected particles, the low energy threshold can be put at 20 keV.

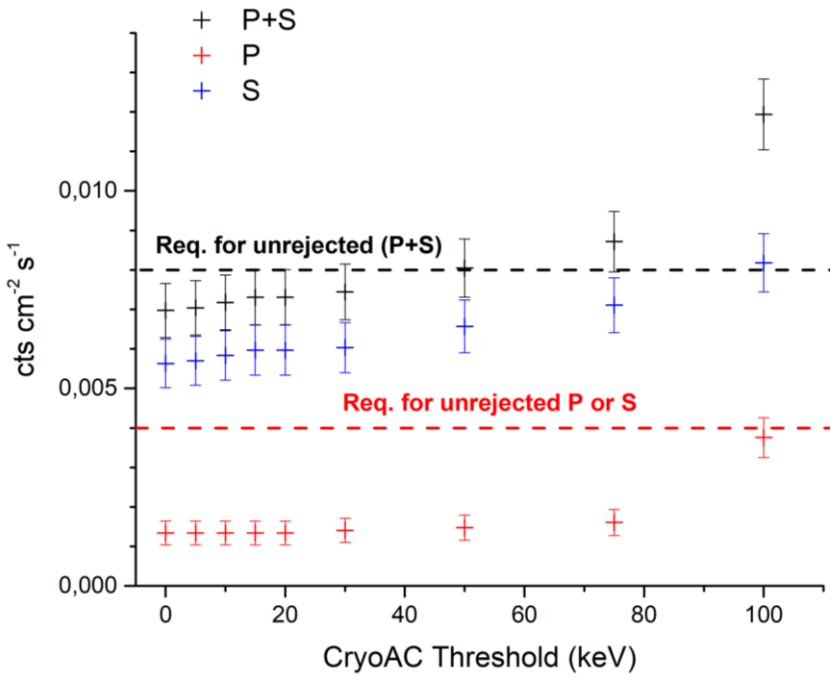

Fig. 4 - The residual NXB (integrated over 2-10 keV bandwidth) vs the CryoAC low energy threshold.

We can now assess the CryoAC detection efficiency, or inefficiency, by evaluating the fraction of particles lost under a generic low energy threshold. The input flux is the expected GCR protons component, thus the result depends on this input. We remark that by using Geant4, all the efficiency, or inefficiency, can be attributed only to the energy deposited on the CryoAC. Again, also here the secondaries drive the trend below the deposited MIP at ~ 150 keV (Fig. 5).

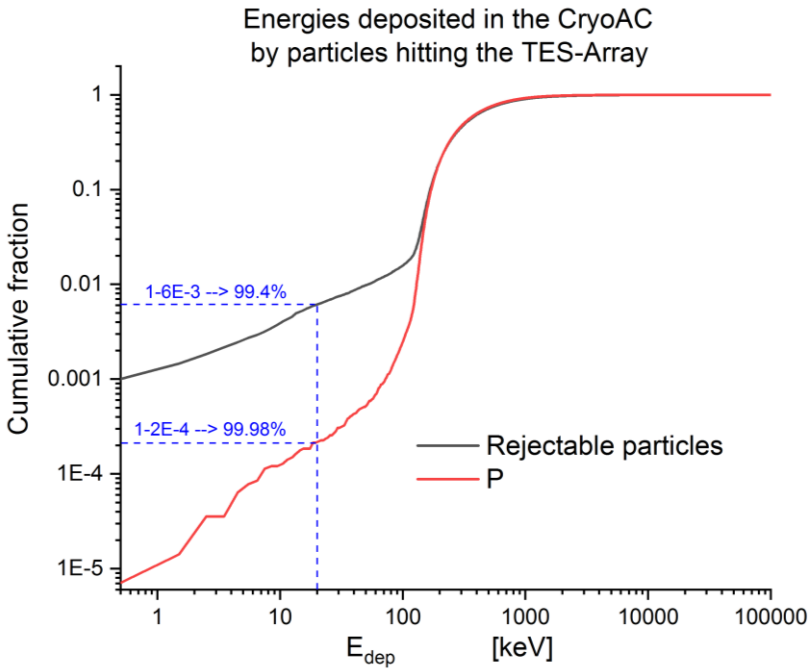

Fig. 5 - CryoAC cumulative distributions of the deposited energies by particles hitting the TES array. The input flux is the expected GCR protons component.

Since the detector cannot distinguish among primaries and secondaries, the total amount has been here renamed as “Rejectable particles”, namely the ones that hit both detectors. From 99.98% detection efficiency due to only primaries, the CryoAC moves to 99.4% for all the Rejectable Particles, for an input spectrum that is the reference GCR protons one.

To conclude this last part of the exercise in re-phrasing this last CryoAC requirement, rather than to provide a detector “detection efficiency” req., it could be more simple to be understood, to emit a requirement on the “low energy threshold” (i.e., 20 keV) which is justified by allocating a fraction of particles that can be admitted to be lost without affecting the NXB to be reached.